Cys; D, Asp; G, Gly; L, Leu; M, Met; R, Arg; S, Ser; T, Thr; V, Val; Y, Tyr) was synthesized and coupled through the cysteine residue to hemocyanin, thyroglobulin, and rabbit serum albumin (RSA). Rabbits were immunized with 25 μg, each, of the peptide-hemocyanin conjugate emulsified in complete Freund's adjuvant and boosted 4 weeks later with 25 μg, each, of the peptide-thyroglobulin conjugate emulsified in incomplete Freund's adjuvant. Specific antibody to peptide was purified by applying antisera to an affinity column made by coupling the peptide-RSA conjugate to Sepharose 4B.

17. HeLa cells grown on cover slips were treated with α-amanitin (20 μg/ml for 4 hours, 40 min) or with actinomycin D (0.5 μg/ml for 1 hour). Treated and untreated cells were fixed, permeabilized, and incubated with a mAb to the large subunit of RNA Pol II (*18*) and with affinity-purified rabbit antibodies to adrenal myosin I (*7*) (both 7 μg/ml, 1 hour). The primary antibodies were visualized with Cy5-conjugated antibodies to mouse IgG and fluorescein isothiocyanate–conjugated antibodies to rabbit IgG (Jackson). Cover slips were mounted using Moviol and examined using a Leica TCS SP laser scanning confocal microscope system.
18. V. T. Nguyen *et al*., *Nucleic Acids Res.* **24**, 2924 (1996).
19. B. Alberts *et al*., *The Molecular Biology of the Cell* (Garland, New York, ed. 3, 1994).
20. F. J. Iborra, A. Pombo, D. A. Jackson, P. R. Cook, *J. Cell Sci.* **109**, 1427 (1996).
21. HeLa cells grown in suspension were treated with α-amanitin or actinomycin D as described (*17*). Treated and untreated cells were pelleted, fixed, and processed for immunoelectron microscopy (*7*). Sections (80 nm) were simultaneously incubated with RNA Pol II mAb (*18*) and with affinity-purified rabbit antibodies to adrenal myosin I (*7*) (both 10 μg/ml, 45 min). The primary antibodies were visualized using 5-nm gold-conjugated antibodies to mouse IgG and 10-nm gold-conjugated antibodies to rabbit IgG (British BioCell International Ltd.). The sections were contrasted with saturated uranyl acetate and examined using a Philips CM 100 electron microscope equipped with a charge-coupled device camera. A statistical analysis of colocalization was performed on 40 random digital EM images per experimental group (63.4 μm^2). Briefly, XY coordinates of all gold particles were recorded and the distances between points *x* and *y*, corresponding to pairs of 5 and 10 nm gold labels in individual images, were quantified. A histogram was generated and confidence intervals of 95% and 99% (*P* values <0.05 and 0.01, respectively) were estimated by Monte Carlo simulations of Poisson process for independent particles (A. A. Philimonenko, J. Janacek, P. Hozak, in preparation).
22. NMIβ was immunoprecipitated from isolated nuclei (*8*) using 20 μg of antibody to NMIβ peptide or 20 μg of the same antibody preadsorbed with 28 μg of peptide. The immunoprecipitates were analyzed by protein immunoblotting with antibody to NMIβ peptide or a mAb to the large subunit of RNA Pol II [S. B. Lavoie, A. L. Albert, A. Thibodeau, M. Vincent, *Biochem. Cell Biol.* **77**, 367 (1999)].
23. An in vitro transcription assay that quantifies transcription by RNA Pol II was performed using a HeLa nuclear extract system as described by the manufacturer (Promega, Madison, WI). Nuclear extract (8 units) treated with RNAguard RNase inhibitor (Pharmacia, Piscataway, NJ) was preincubated (30 min at room temperature) with buffer, 8 μg of affinity-purified antibodies to smooth muscle myosin II [P. de Lanerolle, J. R. Condit Jr., M. Tannenbaum, R. S. Adelstein, *Nature* **298**, 871 (1982)], 0.5 μg of α-amanitin, and either 8 μg of antibody to NMIβ peptide or 8 μg of the same antibody preadsorbed with 11.2 μg of peptide. HeLa template DNA (100 ng) containing the cytomegalovirus immediate early promoter was added and the reaction mixture (25 μl) was made 3 mM $MgCl_2$, 0.4 mM, each, ATP, cytidine 5′-triphosphate, and uridine 5′-triphosphate. Unlabeled guanosine 5′-triphosphate (GTP) (0.04 mM) and [α-^{32}P]GTP (10 μCi) were added and the reaction mixtures were incubated for 30 min at 30°C. The transcription products were separated by 6% acrylamide, 7 M urea denaturing gel electrophoresis, and analyzed using a PhosphorImager.
24. B. Alberts, *Cell* **92**, 291 (1998)
25. O. J. Rando, K. Zhao, G. R. Crabtree, *Trends Cell Biol.* **10**, 92 (2000).
26. H. Yin *et al*., *Science* **270**, 1653 (1995).
27. J. Gelles and R. Landick, *Cell* **93**, 13 (1998).
28. P. R. Cook, *Science* **284**, 1790 (1999).
29. The microsequence of the 120-kD protein can be seen at *Science* Online (www.sciencemag.org/feature/data/1054436.shl).
30. We thank M. Vigneron (Illkirch, France) and M. Vincent (Quebec, Canada) for antibodies to RNA Pol II, and M. L. Chen for assistance with the confocal microscopy. Supported in part by grants from the U.S. Public Health Service to D.F.H. (NIH GM 37537) and to P. de L. (NSF MCB 9631833, NSF INT 9724168, and NIH GM 56489). P.H. is supported by the Grant Agency of the Academy of Sciences (A5039701), by the Grant Agency of the Czech Republic (304/98/1035), and by NSF (USA)/Ministry of Education of the Czech Republic grant ME 143. L.P.-D. and Y.K. were supported by an NIH Training Grant.

24 November 1999; accepted 22 August 2000

Plasma Membrane Compartmentalization in Yeast by Messenger RNA Transport and a Septin Diffusion Barrier

Peter A. Takizawa,[1] Joseph L. DeRisi,[2] James E. Wilhelm,[1] Ronald D. Vale[1,3]*

Asymmetric localization of proteins plays a key role in many cellular processes, including cell polarity and cell fate determination. Using DNA microarray analysis, we identified a plasma membrane protein-encoding mRNA (IST2) that is transported to the bud tip by an actomyosin-based process. mRNA localization created a higher concentration of *IST2* protein in the bud compared with that of the mother cell, and this asymmetry was maintained by a septin-mediated membrane diffusion barrier at the mother-bud neck. These results indicate that yeast creates distinct plasma membrane compartments, as has been described in neurons and epithelial cells.

An important means of achieving asymmetric protein distributions is through the cytoskeleton-dependent localization of cytoplasmic mRNAs (*1*). In *Saccharomyces cerevisiae*, the transcription factor Ash1p accumulates in the daughter cell nucleus, where it represses mating-type switching (*2*, *3*). The asymmetric distribution of Ash1p is created through the transport of *ASH1* mRNA to the bud tip by an actomyosin-driven mechanism (*4*, *5*). Localization of *ASH1* mRNA requires at least three proteins that are physically associated with *ASH1* mRNA: Myo4p (She1p), the myosin motor that transports *ASH1* mRNA along actin filaments to the bud tip; She3p, an adapter that mediates the association between Myo4p and *ASH1* mRNA; and She2p, which is required for the She3p-Myo4p complex to bind *ASH1* mRNA (*6*–*8*). Both She3p and Myo4p localize to the bud tip before *ASH1* mRNA expression (*9*), raising the possibility that other mRNAs are transported in yeast.

To discover other potential localized mRNAs, we identified transcripts that associate with She2p, She3p, and Myo4p using a whole-genome analysis (Fig. 1A). Each of these three proteins was immunoprecipitated from cell extracts using a Myc-epitope tag. Associated RNA was eluted and amplified by reverse transcription followed by polymerase chain reaction (RT-PCR), and the products were fluorescently labeled. An immunoprecipitate from an untagged strain served as a comparative control, and the RT-PCR product from this immunoprecipitate was labeled with a second fluorescent dye. The relative amounts of yeast mRNAs in the She protein versus control immunoprecipitations were determined by hybridization to a DNA microarray containing all *S. cerevisiae* open reading frames. *ASH1* mRNA was enriched in all three immunoprecipitates (2.9-, 2.0-, and 2.2-fold compared with control immunoprecipitates for She2p, She3p, and Myo4p, respectively), validating this approach for identifying other localized mRNAs. Other transcripts that showed a similar enrichment to *ASH1* mRNA (*10*) were then analyzed by fluorescence in situ hybridization (*5*). One of these transcripts, IST2 (increased sodium tolerance) (*11*), showed a localization pattern at the bud tip (Fig. 2A). However, in contrast to *ASH1* mRNA, which is

[1]Department of Cellular and Molecular Pharmacology and [2]Department of Biochemistry/Biophysics, and [3]Howard Hughes Medical Institute, University of California, San Francisco, CA 94143, USA.

*To whom correspondence should be addressed. E-mail: vale@phy.ucsf.edu

expressed only in late anaphase, *IST2* mRNA was localized to the bud tip throughout the cell cycle (Fig. 2A).

To determine whether *IST2* mRNA is localized using a mechanism similar to that of *ASH1* mRNA, we further tested for a physical association between *IST2* mRNA and the She proteins and examined whether localization is disrupted in cells deleted of the *SHE* genes. Quantitative Northern analysis revealed that *IST2* mRNA, like *ASH1* mRNA (*8*), immunoprecipitated with She2p, She3p, and Myo4p (Fig. 1B), confirming the DNA microarray result. Moreover, in *she2*Δ, *she3*Δ, *she4*Δ, and *myo4*Δ cells, *IST2* mRNA was distributed throughout the mother and daughter cell (Fig. 2B). Deletion of *BNI1*, a gene encoding an actin regulatory protein (*12*), caused mislocalization of *IST2* mRNA to the neck, as was observed for *ASH1* mRNA (*4*, *5*). Thus, *IST2* mRNA localization requires the same protein components as *ASH1* mRNA, suggesting that actomyosin-based transport of mRNAs to the distal tip functions throughout the cell cycle.

Expression of a green fluorescent protein Ist2p fusion protein (GFP-Ist2p) from the inducible GAL1 promoter resulted in a fluorescent signal at the plasma membrane (Fig. 3), consistent with sequence predictions indicating the presence of several transmembrane domains in Ist2p (*11*). GFP-Ist2p localized to the mother cell in small-budded cells, but localized to the bud in medium- and large-budded cells (Fig. 3A). The localization of GFP-Ist2p to the bud required the same proteins needed to localize *IST2* mRNA. In cells deleted of *SHE2*, *SHE3*, *SHE4*, or *MYO4*, GFP-Ist2 was localized to the mother cell even in large-budded cells, whereas *bni1*Δ cells contained GFP-Ist2p in both mother cell and bud (Fig. 3B). Thus, the asymmetric distribution of Ist2p to the bud is mediated by the localization of *IST2* mRNA to the distal tip of the bud.

Although GFP-Ist2p was distributed uniformly throughout the bud, the fluorescence signal abruptly diminished at the neck between the mother and daughter cells (Figs. 3 and 4B). Two possible mechanisms could account for the lack of Ist2p signal beyond the neck: Ist2p is anchored in the plasma membrane of the bud, or Ist2p is mobile in the membrane but is prevented from diffusing into the mother cell by a barrier at the neck. To distinguish between these two possibilities, we determined the mobility of GFP-Ist2p within the plasma membrane by fluorescent recovery after photobleaching (FRAP). To eliminate recovery due to newly synthesized protein, GFP-Ist2p was expressed from the inducible GAL1 promoter. Expression was turned off by adding dextrose. A segment of the plasma membrane of a large bud was photobleached for 1 s, and

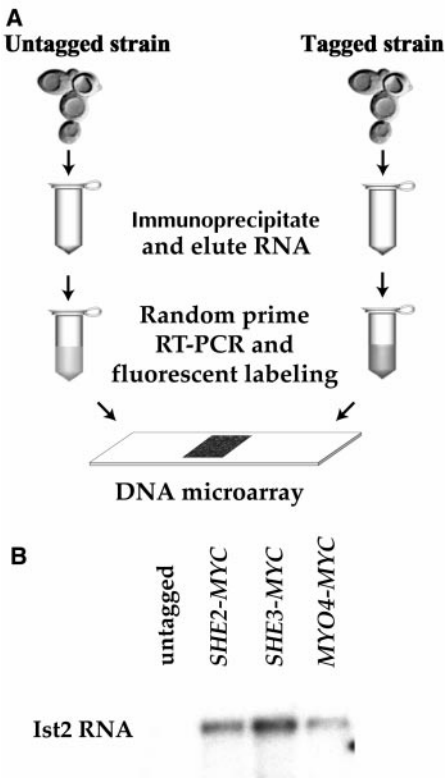

Fig. 1. The *IST2* mRNA is associated with She2p, She3p, and Myo4p. (**A**) Schematic of the DNA microarray procedure used to identify RNAs associated with She2p, She3p, and Myo4p. Tagged strains are *SHE2-13xMYC*, *SHE3-13xMYC*, or *MYO4-13xMYC* in W303 background and were generated as described (*8*). Proteins were immunoprecipitated (*8*), RNA fractions were amplified by RT-PCR, labeled, and analyzed by a DNA microarray (*24*). (**B**) Northern analysis (*8*) of *IST2* mRNA confirms that *IST2* mRNA is enriched in immunoprecipitates of She2p, She3p, and Myo4p.

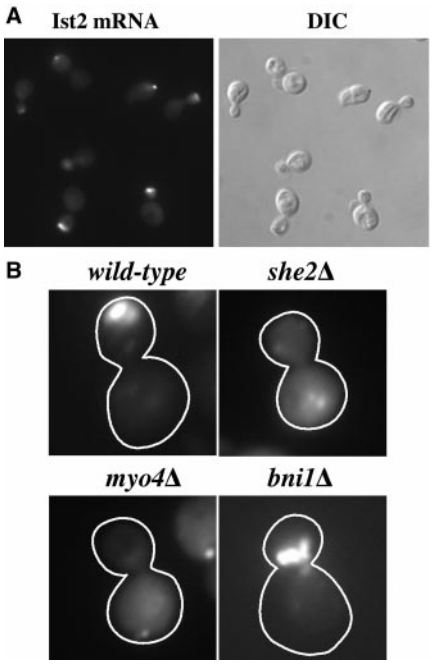

Fig. 2. Localization of *IST2* mRNA to the distal tip of buds requires the She proteins. (**A**) *IST2* mRNA was analyzed in wild-type W303 cells by fluorescence in situ hybridization (*5*). *IST2* mRNA was detected at the distal tip of buds and at the presumptive bud site in unbudded cells. Differential interference contrast (DIC) microscopy reveals the locations of cells and buds. (**B**) *IST2* mRNA was analyzed in wild-type and *she*Δ strains (W303 background) by fluorescence in situ hybridization (*5*). *IST2* mRNA is distributed throughout the mother cell and bud in *she2*Δ and *myo4*Δ cells; *she3*Δ and *she4*Δ cells display a similar *IST2* mRNA distribution as *she2*Δ and *myo4*Δ (*16*). In *bni1*Δ cells, *IST2* mRNA is localized to the neck region. Quantitative analysis revealed that *IST2* mRNA was asymmetrically localized to the bud in more than 95% of wild-type (W303) cells, whereas in examining over 200 *she2*Δ, *she3*Δ, *myo4*Δ, or *she4*Δ cells, an asymmetric distribution of *IST2* mRNA in the bud was never detected. Most (75%) of *bni1*Δ cells contained *IST2* mRNA at the neck; the remaining 25% of cells showed no localized *IST2* mRNA.

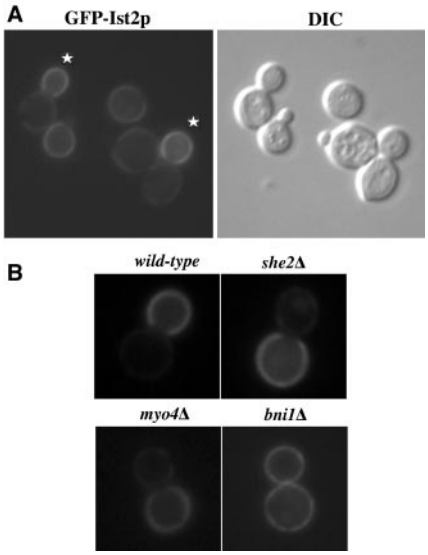

Fig. 3. Asymmetric distribution of GFP-Ist2p in the plasma membrane of buds requires the She proteins. (**A**) GPF-*IST2* was expressed from the galactose promoter in wild-type cells (*25*). GFP-Ist2p was observed in the plasma membrane of the mother cell in unbudded and small-budded cells but was localized to the bud in medium- and large-budded cells (indicated by stars). DIC microscopy reveals the locations of cells and buds. (**B**) Expression of GFP-Ist2p in wild-type and *she*Δ strains reveals that the asymmetric distribution of Ist2p in large-budded cells requires the She proteins. *she3*Δ and *she4*Δ cells show a distribution of GFP-Ist2p similar to that of *she2*Δ and *myo4*Δ (*16*). Quantification of the fluorescence intensities in the mother cell and bud revealed that GFP-Ist2p was enriched 3.5-fold in the bud in W303; 2.2-fold in the mother cell in *she2*Δ; 2.6-fold in the mother cell in *she3*Δ; 2.1-fold in the mother cell in *myo4*Δ; 1.6-fold in the mother cell in *she4*Δ; and 1.1-fold in the bud in *bni1*Δ ($n = 10$).

recovery was monitored every 2 s. The fluorescent signal recovered within 9 s (Fig. 4A), indicating that GFP-Ist2p can diffuse within the plasma membrane of the daughter cell and suggesting that a diffusion barrier at the neck restricts Ist2p to the bud (*13*).

One potential candidate for a diffusion barrier is the septin-based ring filament that forms at the neck during bud growth. The septins are required for cytokinesis, although their precise biological roles are not well defined (*14*). The localization of *IST2* mRNA and protein was examined in cells containing a temperature-sensitive mutation (*cdc12-6*) in the septin gene, *CDC12* (*15*). At both permissive (24°C) and restrictive (37°C) temperatures, *IST2* mRNA was localized to the distal tip of the bud in *cdc12-6* cells (*16*). To determine whether septins affect GFP-Ist2p localization, GFP-Ist2p was expressed at the permissive temperature, protein production was turned off by the addition of dextrose, and then the culture was shifted to the restrictive temperature for 10 min to disassemble the septins (Fig. 4B). At the permissive temperature, 90% of the large-budded wild-type cells displayed an asymmetric distribution of GFP-Ist2p, whereas 52% of the large-budded *cdc12-6* cells contained GFP-Ist2p, predominantly in the bud. Incubation at the restrictive temperature had little effect on GFP-Ist2p localization in wild-type cells (84% of the large-budded cells showed localization to the bud). However, after the 10-min shift to the restrictive temperature, only 12% of the large-budded *cdc12-6* cells contained asymmetrically localized GFP-Ist2p (*17*). The inability of *cdc12-6* cells to maintain the asymmetric distribution of Ist2p at the restrictive temperature suggests that the septins are required to form a barrier at the neck, which prevents Ist2p from diffusing into the mother cell. On the other hand, treatment with the actin-depolymerizing agent, latrunculin-A, did not affect the bud-localized GFP-Ist2p, indicating that actin is not required to maintain GFP-Ist2p in the bud (*17*). The reduction of asymmetrically localized GFP-Ist2p in *cdc12-6* cells at the permissive temperature may result from an imperfect formation of this barrier even at lower temperatures.

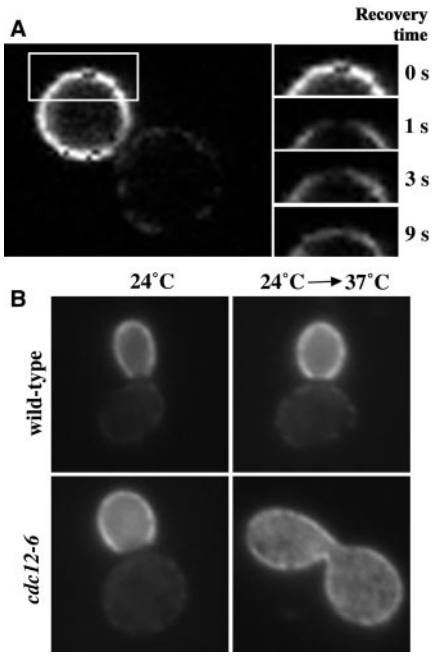

Fig. 4. The GFP-Ist2p fusion protein can diffuse within the plasma membrane of the bud and requires a septin-based diffusion barrier at the neck to maintain asymmetric localization. (**A**) GFP-Ist2p was expressed in wild-type cells, and the expression was then turned off with dextrose. Large-budded cells containing an asymmetric distribution of GFP-Ist2p were subjected to a 1-s photobleach of the GFP signal in the bud (*26*). Time-lapse images were taken before the bleach (0 s), and immediately after photobleaching, to assess the recovery of the fluorescence signal in the photobleached area. Twenty large buds were examined, and all showed a recovery of fluorescence signal in the photobleached area similar to that in surrounding areas within 15 s (*26*). (**B**) Maintenance of bud-localized GFP-Ist2p requires the septins. GFP-Ist2p was expressed from the galactose promoter in wild-type (A364) and *cdc12-6* cells (a temperature-sensitive mutation in one of the septin genes) at the permissive temperature (24°C). Protein expression was turned off by dextrose, and the cultures were then shifted to the restrictive temperature (37°C). The shift in temperature had little effect of GFP-Ist2p in wild-type cells but caused a dramatic decrease in the asymmetric localization of GFP-Ist2p in the septin mutant cell line (*27*).

These results suggest that the asymmetric localization of Ist2p is achieved through transport of *IST2* mRNA to the bud tip by an actomyosin-driven process similar to that described for *ASH1* mRNA. Once *IST2* mRNA is transported and docked at the bud tip, local translation and secretion presumably deliver Ist2p to the plasma membrane of the bud. During this time, turnover diminishes the levels of Ist2p in the mother cell. Maintenance of Ist2p in the bud also requires a septin-mediated diffusion barrier at the neck. It is still unclear whether the septin neck filaments form this barrier or whether they are necessary for localizing other proteins to the neck that act as the diffusion gates.

These findings reveal that yeast has a specialized cytoskeletal architecture at the neck that creates separate plasma membrane compartments in the mother cell and bud that may be important for polarized growth. Septins also are required to maintain the asymmetric distribution of several soluble proteins, such as Myo2p, Sec3p, and Spa2p, that function in polarized growth in the bud (*18*). If these proteins are associated with transmembrane proteins, the septin-mediated barricade of membrane diffusion may provide a mechanism for trapping these proteins within the bud. Diffusion barriers also are vital to the function of higher eukaryotic cells. In epithelia, the tight junctions act as a protein and lipid diffusion barrier that maintains cell polarity (*19*, *20*). An actin-based diffusion barrier was also described in the initial segment of axons in neurons (*21*, *22*), and several distinct compartments also have been described in mammalian sperm (*23*). Very little is known, however, about the components and detailed mechanism of these diffusion barriers in differentiated cells. Genetic approaches in *S. cerevisiae* make this an excellent model system for understanding how the cytoskeleton can restrict the motion of plasma membrane components and create specialized compartments.

References and Notes

1. A. Bashirullah, R. L. Cooperstock, H. D. Lipshitz, *Annu. Rev. Biochem.* **67**, 335 (1998).
2. N. Bobola, R. P. Jansen, T. H. Shin, K. Nasmyth, *Cell* **84**, 699 (1996).
3. A. Sil and I. Herskowitz, *Cell* **84**, 711 (1996).
4. R. M. Long *et al.*, *Science* **277**, 383 (1997).
5. P. A. Takizawa, A. Sil, J. R. Swedlow, I. Herskowitz, R. D. Vale, *Nature* **389**, 90 (1997).
6. E. Bertrand *et al.*, *Mol. Cell* **2**, 437 (1998).
7. S. Munchow, C. Sauter, R. P. Jansen, *J. Cell Sci.* **112**, 1511 (1999).
8. P. A. Takizawa and R. D. Vale, *Proc. Natl. Acad. Sci. U.S.A.* **97**, 5273 (2000).
9. R. P. Jansen, C. Dowzer, C. Michaelis, M. Galova, K. Nasmyth, *Cell* **84**, 687 (1996).
10. A list of all the RNAs that were identified by this procedure is available to *Science* Online subscribers www.sciencemag.org/feature/data/1053179.shl
11. An *IST2* gene deletion enabled cells to grow better than wild-type on medium containing high NaCl (*28*). Sequence analysis of *IST2* has revealed similarities to sodium and calcium channel proteins. For further information see the *Saccharomyces* Genome Database at http://genome-www.stanford.edu/Saccharomyces/; database accession number is S0000290.
12. M. Evangelista *et al.*, *Science* **276**, 118 (1997).
13. To test the possibility that the fluorescence recovery after photobleaching might be due to either new synthesis of GFP-Ist2p or endocytosis of unbleached GFP-Ist2p and exocytosis at the bleached site, we performed the following controls. To control for new synthesis of GFP-Ist2p, GFP-Ist2p was expressed in wild-type cells (*25*) and then 60 μg/ml cycloheximide, a potent inhibitor of protein translation, was added 10 min before examination by FRAP. To control for endocytosis of GFP-Ist2p, 500 μM latrunculin-A, which has been shown to inhibit endocytosis (*29*), was added 10 min before examination by FRAP. Neither cycloheximide nor latrunculin-A had any effect on the fluorescence recovery of GFP-Ist2p after photobleaching, indicating that the recovery was not due to new synthesis of GFP-Ist2p or recycling of unbleached GFP-Ist2p.
14. M. S. Longtine *et al.*, *Curr. Opin. Cell Biol.* **8**, 106 (1996).
15. H. B. Kim, B. K. Haarer, J. R. Pringle, *J. Cell Biol.* **112**, 535 (1991).
16. P. A. Takizawa, J. L. DeRisi, J. E. Wilhelm, R. D. Vale, data not shown.
17. To test the possibility that the mother-cell localization of GFP-Ist2p observed in *cdc12-6* cells at the restrictive temperature might be due to either new synthesis of GFP-Ist2p or endocytosis of existing GFP-Ist2p from the bud, cells were treated with cycloheximide or latrunculin-A before they were shifted to restrictive temperature as described (*13*). Neither cycloheximide nor latrunculin-A had any effect on the mother-cell localization of GFP-Ist2p in *cdc12-6* cells at the restrictive temperature, indicating that this mislocalization of GFP-Ist2p was not due

to new protein synthesis or recycling from the bud. Also, latrunculin-A (20 min, 500 μM) did not cause a shift in GFP-Ist2p from bud to mother cell in wild-type or *cdc12-6* cells at the permissive temperature. Thus, actin is not required to maintain GFP-Ist2p in the bud.
18. Y. Barral, V. Mermall, M. S. Mooseker, M. Snyder, *Mol. Cell* **5**, 841 (2000).
19. E. Rodriguez-Boulan and W. J. Nelson, *Science* **245**, 718 (1989).
20. M. S. Balda *et al.*, *J. Cell Biol.* **134**, 1031 (1996).
21. B. Winckler, P. Forscher, I. Mellman, *Nature* **397**, 698 (1999).
22. D. Zhou *et al.*, *J. Cell Biol.* **143**, 1295 (1998).
23. C. L. Nehme, M. M. Cesario, D. G. Myles, D. E. Koppel, J. R. Bartles, *J. Cell Biol.* **120**, 687 (1993).
24. Immunoprecipitation of She2p-myc, She3p-myc, Myo4p-myc and untagged control were performed as described (*8*). RNA fractions were prepared from the immunoprecipitates by extraction of the eluate with phenol/chloroform and precipitation with ethanol. The RNA was reverse-transcribed with Superscript II (Life Technologies, Rockville, MD) according to the manufacturer's instructions and using the primer, GTTTCCCAGTCACGATC$(N)_6$. After the reverse transcription, the reactions were incubated for 2 min at 94°C and then held at 8°C. Four units of T7 sequenase (Amersham Pharmacia, Uppsala) was added, and the reaction was ramped to 37°C at 0.1°C per second and then held for 8 min at 37°C. The sequenase step was repeated once. A portion of the reaction was then amplified by PCR using the sequence-specific end of the first primer. The resulting amplified DNA was fluorescently labeled by a subsequent round of PCR (25 cycles) in presence of either Cy3-dUTP or Cy5-dUTP (Amersham). These reactions were purified using the QiaQuick PCR purification kit (Qiagen, Valencia, CA), and then applied to the DNA microarray. DNA microarrays were fabricated and hybridized as described (*19*). Genepix software (Axon Instruments, Forest City, CA) was used for image analysis and quantification. DNA microarray analysis was performed in duplicate.
25. The *IST2* gene was tagged with the method described in (*30*). All strains were derived from w303. Strains containing pGAL-GFP-*IST2* were grown in rich medium (YP) containing 2% raffinose. At absorbance of 0.5 U, galactose was added to 2%, and the cultures were incubated for 1 to 1.5 hours at 30°C. Cells were fixed with 4% formaldehyde and then examined on a Zeiss Axioplan fluorescence microscope. Images were captured with a CCD camera and processed with Adobe Photoshop.
26. To perform FRAP, wild-type, W303 cells containing pGAL-GFP-*IST2* cells were induced (*25*) and then incubated in 2% dextrose for 10 min to turn off production of GFP-Ist2p. Cells were examined on a Leica TCS NT confocal microscope, and a portion of a large bud was photobleached for 1 s. An image was captured immediately after the photobleaching and then every 2 s thereafter. Images were analyzed using NIH Image and Adobe Photoshop.
27. To analyze the effect of a septin mutant on the localization of GFP-Ist2p, *cdc12-6* and its parental strain, A364, containing pGAL-GFP-*IST2* were grown in rich medium (YP) with 2% raffinose at 24°C until absorbance 0.5 U. Galactose was added to 2%, and the cultures incubated for 1 hour at 24°C. Dextrose was added to 2%, and the cultures were incubated for 10 min at 24°C. A sample was removed, and the cultures were shifted to 37°C for 10 min, after which time a second sample was taken. All samples were fixed in 4% formaldehyde and examined as described (*25*). Images were captured and processed as described. Large-budded cells (100 in each sample) were analyzed and counted for asymmetric GFP-Ist2p.
28. K. D. Entian *et al.*, *Mol. Gen. Genet.* **262**, 683 (1999).
29. D. Drubin, personal communication.
30. M. S. Longtine *et al.*, *Yeast* **14**, 953 (1998).
31. We thank A. Sil, I. Herskowitz, and C. Takizawa for critical review of the manuscript. We would also like to thank members of the Herskowitz, Walter, Murray, and O'Shea laboratories for their help in producing the microarrays used in this study. This work was supported in part by National Institutes of Health grant 38496 (R.D.V.), a grant from the Jane Coffin Childs Memorial Fund for Medical Research Fellowship (P.A.T.), and the Sandler Family (J.D.R).

15 June 2000; accepted 24 August 2000

Molecular Analysis of *FRIGIDA*, a Major Determinant of Natural Variation in *Arabidopsis* Flowering Time

Urban Johanson,[1]* Joanne West,[1]† Clare Lister,[1] Scott Michaels,[2] Richard Amasino,[2] Caroline Dean[1]‡

Vernalization, the acceleration of flowering by a long period of cold temperature, ensures that many plants overwinter vegetatively and flower in spring. In *Arabidopsis*, allelic variation at the *FRIGIDA* (*FRI*) locus is a major determinant of natural variation in flowering time. Dominant alleles of *FRI* confer late flowering, which is reversed to earliness by vernalization. We cloned *FRI* and analyzed the molecular basis of the allelic variation. Most of the early-flowering ecotypes analyzed carry *FRI* alleles containing one of two different deletions that disrupt the open reading frame. Loss-of-function mutations at *FRI* have thus provided the basis for the evolution of many early-flowering ecotypes.

A requirement for vernalization—the acceleration of flowering that occurs during a 3- to 8-week period of cold temperature (4°C)—has been bred in many crops to produce winter/spring varieties. Vernalization requirement is also a major factor in determining flowering time in *Arabidopsis thaliana* ecotypes. Despite the large number of genes known to control flowering time (*1*), the vernalization requirement segregates as a single gene trait (*2–6*) mapping to the *FRIGIDA* (*FRI*) locus (*7*). This locus was first described by Napp-Zinn (*8*), who analyzed the progeny of a cross between the late-flowering ecotype Stockholm and the early-flowering ecotype Li5. The action of an active *FRI* allele depends on an active *FLC* allele (*9, 10*).

To analyze the molecular basis of the allelic variation at *FRI*, we cloned the gene using map-based techniques (Fig. 1) (*11*). *FRI* is a single-copy gene in the *Arabidopsis* genome and encodes a predicted open reading frame (ORF) of 609 amino acids (GenBank accession numbers: genomic *FRI*, AF228499; cDNA, AF228500). The predicted protein shows no significant match to any protein or protein domain of known function in available databases. The *FRI* protein is predicted to contain coiled-coil domains in two positions (between amino acids 55 to 100 and 405 to 450, respectively). *FRI* has been shown to increase RNA levels of *FLC*, which encodes a MADS-box protein likely to act as a transcriptional repressor (*12, 13*). Whether the predicted coiled coils in the FRI protein are important for this function remains to be tested.

The rapid-cycling ecotypes Columbia (Col) and Landsberg *erecta* (L*er*) carry recessive *FRI* alleles. To analyze the basis of the recessivity, we compared ~3.6 kb of genomic sequence from the dominant H51 [a derivative of the late-flowering ecotype Stockholm (*8*)] *FRI* allele with the same region from Col and L*er*. Ten polymorphisms were found between H51 and Col. Two result in amino acid differences ($Gly^{146} \rightarrow Glu$ and $Met^{148} \rightarrow Ile$, respectively, the former resulting in loss of a Bsm FI restriction site); another is a 16–base pair (bp) deletion at the end of exon 1, which changes the reading frame and terminates the ORF immediately at the beginning of exon 2 (Fig. 2).

Three differences were detected between H51 and L*er* *FRI* alleles: two single-base changes that do not alter the ORF, and a 376-bp deletion combined with a 31-bp insertion that disrupts the beginning of the ORF, removing the putative translation start codon (Fig. 2). The additional 31 bp appear to

[1]Department of Molecular Genetics, John Innes Centre, Norwich NR4 7UH, UK. [2]Department of Biochemistry, University of Wisconsin, Madison, WI 53706, USA.

*Present address: Department of Plant Biochemistry, Lund University, Post Office Box 117, SE-221 00 Lund, Sweden.

†Present address: Department of Plant Sciences, University of Cambridge, Cambridge CB2 3EA, UK.

‡To whom correspondence should be addressed. E-mail: caroline.dean@bbsrc.ac.uk